How vegetation impacts affect climate metrics for ozone precursors

W. J. Collins,[1] S. Sitch,[2] and O. Boucher[1]

Received 12 March 2010; revised 25 August 2010; accepted 8 September 2010; published 9 December 2010.

[1] We examine the effect of ozone damage to vegetation as caused by anthropogenic emissions of ozone precursor species and quantify it in terms of its impact on terrestrial carbon stores. A simple climate model is then used to assess the expected changes in global surface temperature from the resulting perturbations to atmospheric concentrations of carbon dioxide, methane, and ozone. The concept of global temperature change potential (GTP) metric, which relates the global average surface temperature change induced by the pulse emission of a species to that induced by a unit mass of carbon dioxide, is used to characterize the impact of changes in emissions of ozone precursors on surface temperature as a function of time. For NO_x emissions, the longer-timescale methane perturbation is of the opposite sign to the perturbations in ozone and carbon dioxide, so NO_x emissions are warming in the short term, but cooling in the long term. For volatile organic compound (VOC), CO, and methane emissions, all the terms are warming for an increase in emissions. The GTPs for the 20 year time horizon are strong functions of emission location, with a large component of the variability owing to the different vegetation responses on different continents. At this time horizon, the induced change in the carbon cycle is the largest single contributor to the GTP metric for NO_x and VOC emissions. For NO_x emissions, we estimate a GTP_{20} of −9 (cooling) to +24 (warming) depending on assumptions of the sensitivity of vegetation types to ozone damage.

Citation: Collins, W. J., S. Sitch, and O. Boucher (2010), How vegetation impacts affect climate metrics for ozone precursors, *J. Geophys. Res.*, *115*, D23308, doi:10.1029/2010JD014187.

1. Introduction

[2] Short-lived pollutants (lifetimes around a decade or less) are increasingly being recognized as important contributors to climate change and potential targets for climate mitigation policies [*Jackson*, 2009]. Methane is currently included in the Kyoto basket of species, whereas other ozone precursor species are typically included in air quality mitigation strategies such as the Gothenburg Protocol [*ApSimon et al.*, 2009]. It is therefore important to know what implications these and future air quality controls will have on climate on different timescales. *Raes and Seinfeld* [2009] suggested that air pollution control measures combined with an underlying CO_2 trend could lead to rates of warming of nearly 0.4 K/decade between 2000 and 2030.

[3] Although many pollutants (such as CO_2) directly lead to a radiative impact on the atmosphere, others, such as ozone precursors, have more complex climate impacts. Emissions of ozone precursors [oxidized nitrogen (NO_x), volatile organic compounds (VOCs), and carbon monoxide (CO)] have little or no direct radiative impact, but they react in the atmosphere to affect the concentrations of compounds that do. Principally, they form ozone in the troposphere, where it acts as greenhouse gas, and either increase (NO_x) or decrease (VOCs and CO) the removal of methane from the atmosphere. Recently *Shindell et al.* [2009] showed that there are further effects to be considered because these ozone precursor species can also indirectly affect the production of sulfate and nitrate aerosols, which contribute to cool the climate.

[4] In this paper we focus on quantifying a further indirect effect whereby the generation of surface ozone pollution can damage vegetation, decreasing the ability of plants to remove CO_2 from the atmosphere. The reduction in removal of CO_2 can be considered an equivalent emission. *Sitch et al.* [2007] found that this equivalent CO_2 emission could have a radiative impact comparable to the direct impact of the ozone itself when comparing 2000 and 2100 (SRES A2) conditions against that of the year 1900. Here we take the Sitch et al. study further by quantifying how the vegetation damage by ozone affects the climate metrics for ozone precursor emissions.

[5] When comparing the climate impacts of different compounds, various measures are used. The radiative forcing is a direct function of the atmospheric concentration of a species and thus dependent on the emission history [e.g., *Forster et al.*, 2007, Figure 2.21], whereas the global warming potential (GWP) and global temperature change potential (GTP) are both related to the response to a pulse emission [*Shine et al.*, 2007]. Below we calculate for the first time the contribution of the damaging effects of ozone on vegetation to the GTPs for ozone precursors. We choose

[1]Met Office Hadley Centre, Exeter, UK.
[2]School of Geography, University of Leeds, Leeds, UK.

Table 1. PFT-Specific Ozone Exposure Parameters[a]

	BT	NT	C3	C4	Shrub
F_{O3crit} (nmol m^{-2} s^{-1})	1.6	1.6	5.0	5.0	1.6
High a ($mmol^{-1}$ m^{-2})	0.15	0.075	1.40	0.735	0.10
Low a ($mmol^{-1}$ m^{-2})	0.04	0.02	0.25	0.13	0.03

[a]Used in the relationship between fractional reduction in plant photosynthesis (F) and ozone uptake above a critical threshold ($UO_{>FO3crit}$), where $F = 1 - aUO_{>FO3crit}$. Values for broad-leaved tree (BT) and needle-leaved tree (NT) calibrated to the work of *Karlsson et al.* [2004]. High and low plant ozone sensitivity parameter a calibrated against regressions for "birch, beech" and "oak," respectively. Parameters for C3 and C4 grass (C3, C4) are calibrated against data from the work of *Pleijel et al.* [2004], with high and low plant ozone sensitivity parameter a calibrated against regressions for "spring wheat" and "potato," respectively. Parameters a for shrub are calibrated as for BT. In the absence of data, the low conifer parameterization is assumed 3.8 times less sensitive than the high parameterization (corresponding to the same ratio for BT). For shrubs we assume the same plant-ozone sensitivity as for BT.

the GTP because it relates directly to the expected change in surface temperature.

2. Model Descriptions

[6] This section describes the three models used in the three stages of the calculations. First a chemistry model (STOCHEM) is run with different emission reductions; the ozone outputs are then used in a terrestrial carbon cycle model (the Joint UK Land Environment Simulator, JULES); and finally a simple climate box model is used to simulate the resulting temperature changes.

2.1. Chemistry Model

[7] The chemistry model used for this study is the STOCHEM Lagrangian tropospheric chemistry model, embedded within an atmosphere-only version (HadGAM1) of the Hadley Centre's climate model HadGEM1 [*Johns et al.*, 2006] with a 30 min coupling step. Both HadGAM1 and STOCHEM are configured here to have a horizontal resolution of 3.75° × 2.5°. STOCHEM is described in detail elsewhere [*Collins et al.*, 2003, and references therein] and has been compared against other models and measurements, for example, by *Stevenson et al.* [2006], *Dentener et al.* [2006], and *Shindell et al.* [2006]. The performance of the ozone simulations for Europe and North America was recently assessed against the surface observations by *Fiore et al.* [2009], with more detail available on the HTAP website (http://htap.icg.fz-juelich.de/data/ExperimentSet1). The STOCHEM model predictions compared well against observations and were found to be within the range of the other model predictions.

2.2. Terrestrial Carbon Cycle Model

[8] We calculate the impact of the ozone damage on terrestrial carbon using the JULES model, which comprises the MOSES surface exchange scheme [*Essery et al.*, 2003] coupled to the TRIFFID dynamic vegetation model [*Cox*, 2001]. JULES includes a coupled representation of leaf photosynthesis and stomatal conductance. This scheme has been modified to include plant ozone damage, assuming a suppression of net leaf photosynthesis by ozone that varies proportionally to the ozone flux through stomata above a specified critical ozone deposition flux [*Sitch et al.*, 2007]. Net photosynthesis is modified by a factor that accounts for both plant ozone uptake and plant-specific sensitivities to ozone uptake.

[9] Data from field observations [*Pleijel et al.*, 2004; *Karlsson et al.*, 2004] are used to calibrate plant-ozone effects for the five plant functional types (PFTs) described by JULES. A "high" and "low" parameterization is chosen for each PFT to represent uncertainty in the responses of different plant species to ozone deposition [*Sitch et al.*, 2007]. JULES represents the carbon allocation, plant growth, PFT competition, and turnover of carbon from the living plant tissues into a one-pool soil carbon model. Therefore, JULES is able to simulate the impact of O_3 on plant photosynthesis and land carbon sequestration. PFT-specific ozone exposure parameters are given in Table 1. Although grasses are assumed to have a higher critical threshold for ozone exposure, they are also more sensitive to an ozone dose above the critical threshold than trees. Therefore, grasses may become more sensitive to ozone exposure than trees at high ozone concentrations. In addition, differences in the turnover of carbon in biomass are PFT-dependent. Therefore, PFT composition will affect the magnitude and duration of the system perturbation to ozone, which are crucial when determining the climate impact of plant O_3 exposure.

[10] As described by *Gedney et al.* [2006], this study uses the 0.5° resolution observational data set from the Climate Research Unit, which contains monthly temperature (mean and diurnal range), humidity, cloud cover, and precipitation (amount and daily frequency). Empirical formulations are used to derive shortwave and longwave radiation from the Climate Research Unit data set. All monthly forcing data are regridded onto a 2.5° × 3.75° grid and disaggregated to hourly data, the resolution at which JULES is run.

2.3. Simple Climate Model

[11] We base our analysis of the global surface temperature impacts on simple carbon cycle and climate models from the work of *Boucher and Reddy* [2008]. These models use impulse response functions to describe the evolution of the atmospheric CO_2 concentration and global surface temperature in response to CO_2 emissions and are repeated below. The parameters in these simple models are derived from simulations with more complex chemistry and climate models. We appreciate that this approach is very simple; however, we believe it is sufficient in the current context to support our conclusions. The fraction of CO_2 remaining in the atmosphere for a pulse emission is given by $f = 0.217 + 0.259 \exp(-t/172.9) + 0.338 \exp(-t/18.51) + 0.186 \exp(-t/1.186)$.

[12] The climate impulse response function is given by $\delta T(t) = 0.631 \exp(-t/8.4) + 0.429 \exp(-t/409.5)$ in K W^{-1} m^2. In both formulas, t is in years. The equilibrium climate sensitivity is thus 1.06 K W^{-1} m^2.

3. Model Experiments and Results

3.1. Chemistry Modeling

[13] The experimental method is designed to attribute a climate forcing to different ozone precursor emissions from different continents in the Northern Hemisphere and, in particular, to quantify the contribution from ozone damage to vegetation. It follows the procedure for the HTAP experiments [*Keating and Zuber*, 2007], whereby emissions of

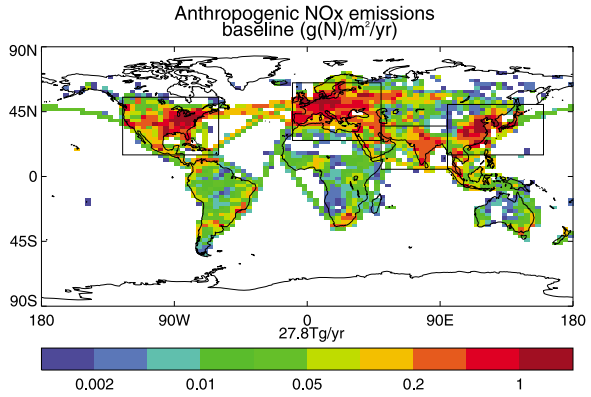

Figure 1. Anthropogenic NO_x emissions used in the control experiment. The boxes illustrate the regions over which the emissions are reduced by 20%.

anthropogenic ozone precursors (NO_x, VOCs, and CO) are separately reduced from a baseline case over four continental regions (North America, Europe, East Asia, and South Asia) by 20%. These continental reductions are performed on a rectangular latitude-longitude box and include any (mainly coastal) shipping emissions within that box. An additional experiment was carried out where global shipping NO_x emissions were decreased by 20%. Only a NO_x reduction experiment was carried out for shipping because the shipping VOC and CO emissions have much less impact. In each of the aforementioned experiments, the methane concentration was fixed to be 1760 ppbv throughout the troposphere. For the methane experiment, the methane concentration, rather than the emission, was reduced by 20%, following the HTAP protocol. Thus, a grand total of 14 perturbations were run on the control experiment. The baseline emissions used the EDGAR3.2 data set [*Olivier and Berdowski*, 2001] for the year 2000 [*Stevenson et al.*, 2006]. The shipping emissions in this data set are relatively simplistic, as discussed by *Eyring et al.* [2007] and *Collins et al.* [2009]. The NO_x baseline emissions are shown in Figure 1. Natural emissions of soil NO_x and biomass burning were as described by *Stevenson et al.* [2006]. Emissions of lightning NO_x were parameterized according to the work of *Price and Rind* [1992], giving 5.8 Tg(N)/yr in this experiment. The interactive isoprene emissions [*Sanderson et al.*, 2003] amounted to 585 Tg/yr.

[14] The STOCHEM chemistry model was run for 28 months for each case. Only the last 12 months of each run are used. The model is embedded in a free-running atmosphere-only general circulation model (GCM) using sea surface temperatures and sea ice fields appropriate for a mid-1990s climate. The chemistry fields have no impact on the climate in this configuration, so the meteorology was identical for each perturbation run. Therefore, we can be sure that any differences in the ozone generated are attributed solely to the emission perturbations and not to the meteorology. Although the sensitivity of the surface ozone to emission perturbations can vary from year to year, the resulting uncertainty is small compared to the uncertainty in the plant responses.

[15] The boreal spring (March, April, May) is chosen to illustrate the impacts of NO_x emissions in Figure 2 because this is the start of the growing season in many ecosystems. The geographical distribution of impacts from changes to the VOC emissions (not shown) is similar to that from NO_x. The impacts from CO emissions (not shown) are more spread out. Although the change in methane was applied uniformly, the surface ozone response was largest over regions of high NO_x emissions.

[16] The impacts of all the emission reductions on the ozone burden and methane lifetime are shown in Table 2. The ozone surface concentrations and tropospheric burdens calculated in Table 2 are for the year of the emissions change and do not take into account the secondary, long-term impact on ozone via changes in methane. Through changes to the methane lifetime, the ozone will continue to respond to the emission perturbation even after its concentrations have reverted to the baseline values. This is taken into account in the climate forcing calculations described in section 3.3.

3.2. Terrestrial Carbon Cycle Modeling

[17] Here we take the surface ozone changes discussed in the previous section and use these to quantify the resulting impacts on the terrestrial carbon cycle. The ozone simulations from section 3.1 are effectively equilibrium simulations because the ozone adjusts rapidly to the changed precursor emissions. To calculate climate impacts it is useful to simulate responses to an emission reduction pulse. We do this by using the steady state perturbed ozone for 1 year as a pulse. The surface ozone concentrations from all the experiments are archived as monthly averages.

[18] JULES is first run from 1901 to 2000 with observed fields of changing climate, atmospheric CO_2 concentration, and simulated O_3 concentrations. Annually varying O_3 fields are derived by interpolating preindustrial and present-day (control) simulated concentration fields. JULES is then run for a further 50 years for the ozone pulse experiment with fixed year 2000 climatology and atmospheric CO_2 concentration throughout. For the first year of the short-lived precursor experiments (i.e., not methane), the perturbed ozone concentrations are used, whereas the ozone concentrations revert to the control values (present-day concentrations) for the subsequent 49 years. These runs are compared to the control case in which the control ozone concentrations are used for all 50 years. In this way we can diagnose the effect of a 1 year pulse of NO_x emission reductions on the terrestrial carbon cycle. We have also created a "four-continents" simulation, where we have summed the ozone responses to the four continental area perturbations. This is done separately for NO_x, VOCs, and CO, and the total ozone perturbations are applied to JULES. This procedure assumes that the responses to the emission perturbations are linear. A sensitivity test showed that nonlinearity was of the order of 1%.

[19] To represent a 1 year methane emission reduction pulse, the ozone response from the methane experiment described in section 3.1 was used. For the first year of the run, the ozone perturbation was scaled by 0.5 to represent the average of a linear decrease in methane over the first year. In subsequent years, the ozone perturbation was scaled by $e^{-t/12.4}$, where t is the years since the start of the integration. Note that the ozone perturbation is of smaller magnitude for the first year than for the following few years.

[20] Figure 3 follows the surface ozone changes from the NO_x reduction experiments through to the impacts on the

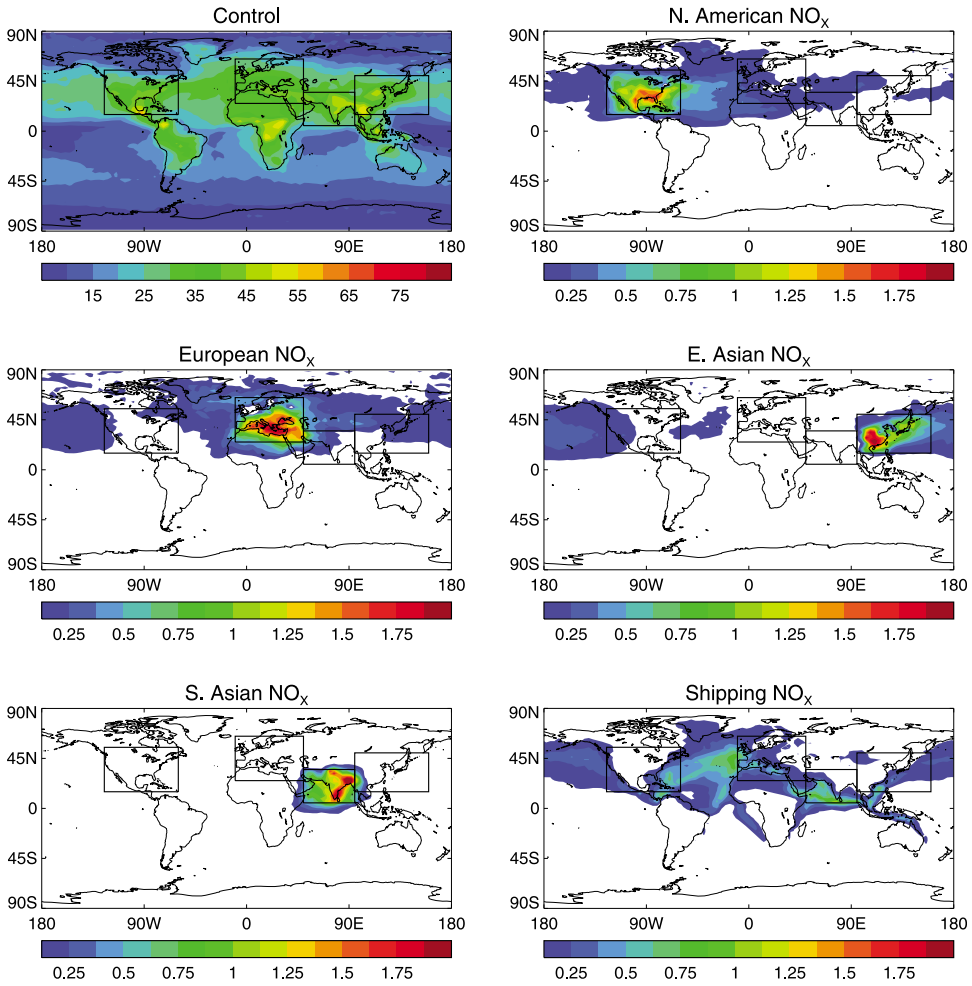

Figure 2. March, April, and May averaged surface ozone concentration (ppbv) for the control simulation, and the simulated decreases due to the 20% reductions in NO_x emissions.

land carbon budget, defined as the sum of the vegetation and soil carbon budgets. The soil carbon budget dominates this sum; results for the vegetation and soil budgets separately follow a similar pattern. The change in land carbon is shown for the year following the emission reduction pulse (i.e., the second year of the experiment). Again, the impacts are closely tied to the region of emission change. In particular, it is interesting to note that the impacts of the European changes are generally confined to that region and seem not to affect the regions of large biomass in the Siberian forests.

[21] The time evolution of the change in land carbon from the NO_x experiments is shown in Figure 4. In this and later figures, we have normalized the data by a +1 Tg change in emission. Thus, the sign of the change is such that a positive emission pulse (and hence increase in surface ozone) leads to an increased impact of ozone on plant productivity and hence a decrease in land carbon storage. There is a decrease in the land carbon storage after the first year of the experiment because of the higher ozone concentrations. After reverting to the unperturbed concentrations, the land carbon storage returns to the control value with different decay times for different source regions. The carbon perturbation decays more rapidly in (South and East) Asian regions than in North

Table 2. Change in Tropospheric Ozone Burden, Methane Lifetime Due to the OH Reaction, and the Total Methane Lifetime Including Dry Deposition and Stratospheric Removal for the 15 Experiments of This Study[a]

Experiment	ΔO_3 (Tg)	$\tau_{CH_4\,OH}$ (yr)	τ_{CH_4} (yr)
Control	(247.12)	10.933	9.430
N. America NO_x	−0.68	10.983	9.467
Europe NO_x	−0.42	10.967	9.455
E. Asia NO_x	−0.56	10.974	9.460
S. Asia NO_x	−0.35	10.965	9.453
Shipping NO_x	−0.54	10.984	9.467
N. America VOC	−0.39	10.923	9.422
Europe VOC	−0.35	10.916	9.417
E. Asia VOC	−0.36	10.922	9.421
S. Asia VOC	−0.16	10.923	9.422
N. America CO	−0.18	10.906	9.409
Europe CO	−0.11	10.916	9.417
E. Asia CO	−0.17	10.906	9.409
S. Asia CO	−0.11	10.916	9.417
Methane	−5.69	10.337	8.983

[a]For the control simulation the total ozone burden is shown rather than the change.

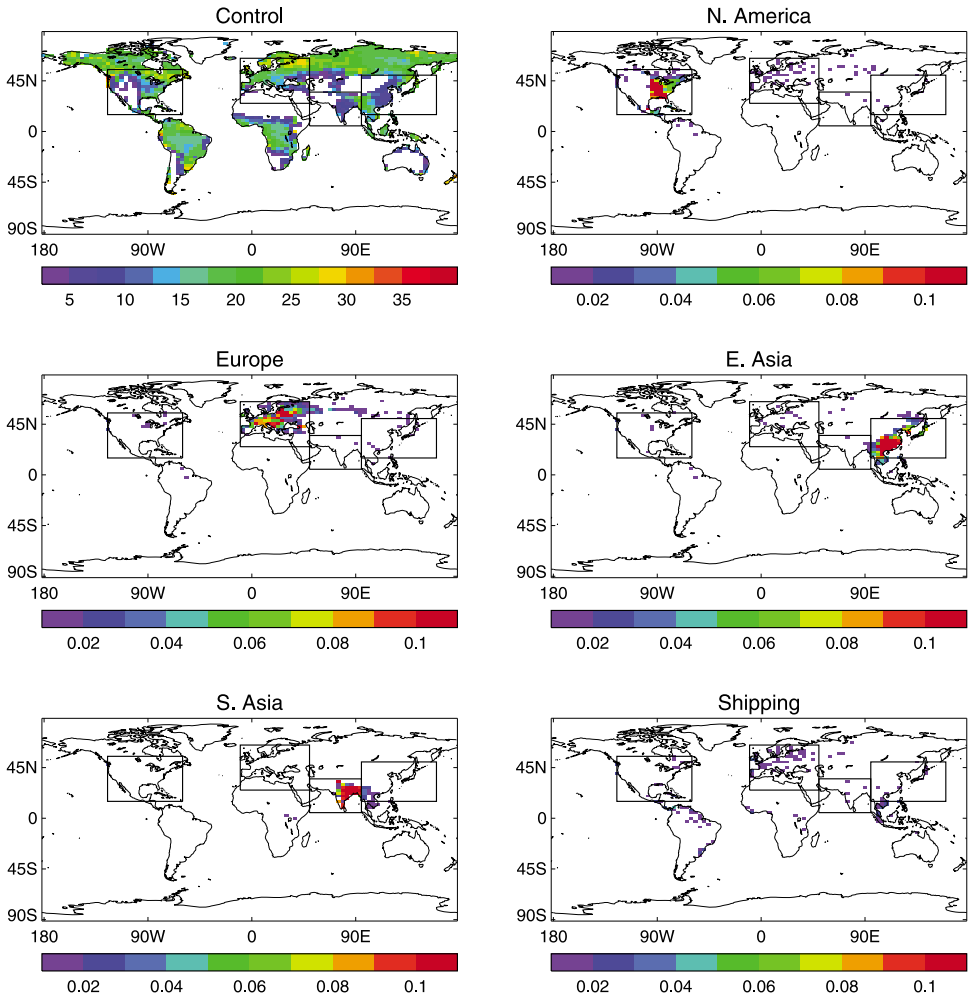

Figure 3. Land carbon store (kg C m^{-2}) for the control experiment and change in land carbon store averaged over year 2 following the regional NO_x emission reductions prescribed in year 1.

America and Europe because of the faster soil respiration and the more rapid turnover of vegetation. After 50 years, the perturbation has declined by roughly a factor of 10 in the case of North America and Europe, and over a factor of 30 in the case of South and East Asia. Shipping NO_x generally has less of an impact on the land carbon store than continental sources.

3.3. Analytical Climate Model

[22] In this section, we take the ozone burden and methane lifetime changes calculated in section 3.1 along with the change in terrestrial carbon storage from section 3.2 to simulate the time evolutions and consequent radiative forcings of ozone, methane, and carbon dioxide following the emission reduction pulses.

[23] To keep a consistent climate, JULES was configured with a fixed atmospheric CO_2 concentration and so could not be used to provide impacts of ozone on atmospheric CO_2. An equivalent change in CO_2 emissions can, however, be inferred from the change in land carbon storage in JULES. Land carbon storage values beyond the end of the 50 year

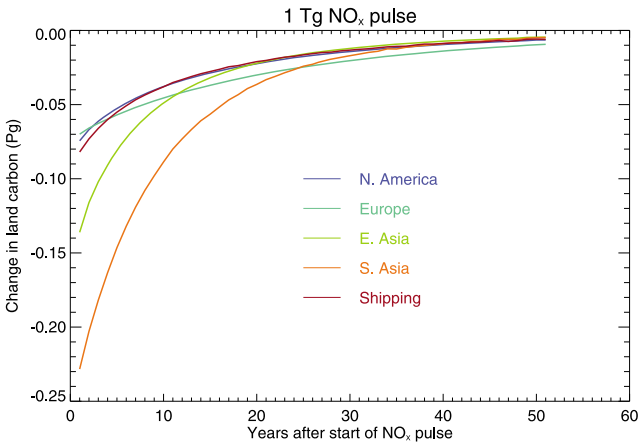

Figure 4. Change in land carbon at the end of each year following 1 year NO_x emission pulses. Values are for the case of high sensitivity of vegetation to ozone.

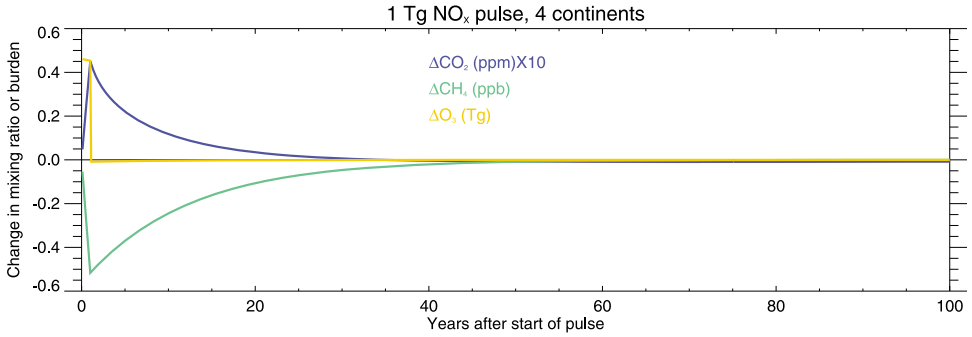

Figure 5. Change in the atmospheric concentrations of CO_2 and CH_4, and the tropospheric burden of O_3 due to a 1 year pulse in NO_x emissions over the four continental regions. Values are for high sensitivity of vegetation to ozone.

JULES run were extrapolated using an exponential decay with a 25 year e-folding time. During the first year of reduced ozone damage, there is a strong uptake (negative emission) of CO_2, followed by a gradual reemission in subsequent years. An impulse response function as described in section 2 is used to convert this to CO_2 concentrations.

[24] The emission reductions also perturb the atmospheric lifetime of methane. NO_x reductions increase the lifetime, and VOC and CO reductions decrease the lifetime (see Table 2). In the chemistry model, the methane mixing ratio was held constant (1760 ppbv) for the ozone precursor experiments, so, for the purposes of the climate impact, the methane concentrations are calculated analytically. During the first year of the perturbation, the methane starts to evolve toward a new equilibrium because of the changed lifetime $CH_{4eqm} = CH_{4,0}(\tau_1/\tau_0)^f$, where f is the feedback factor [*Prather et al.*, 2001], equal to 1.28 in the STOCHEM model; τ_0 is the control lifetime; τ_1 is the methane lifetime with perturbed emissions (from Table 2); and $CH_{4,0}$ is the control value (1760 ppbv). After the first year, methane then reverts to the control value with the atmospheric relaxation timescale $\tau_0 f$. Hence,

$$CH_4 = CH_{4,0} + \left(CH_{4eqm} - CH_{4,0}\right)\left(1 - \exp(-t/\tau_1 f)\right) \quad \text{for } t < 1,$$

$$CH_4 = CH_{4,0} + \left(CH_{4eqm} - CH_{4,0}\right)\left(1 - \exp(-1/\tau_1 f)\right) \cdot \exp(-(t-1)/\tau_0 f) \quad \text{for } t > 1,$$

where t, τ_0, and τ_1 are in years.

[25] For the purpose of estimating the ozone radiative forcing, the annual mean tropospheric burden is used. It is assumed that the ozone responds instantaneously to the emission perturbation; hence, the perturbed burden is used for the first year and the control burden is used for all subsequent years. An additional term is added to the ozone burden to account for the impact of methane changes by scaling the methane change ($CH_4 - CH_{4,0}$) by the ozone sensitivity to methane. This sensitivity was calculated from the 80% methane run to be 0.016 Tg (O_3)/ppbv (CH_4). The land carbon perturbation owing to this additional ozone term is also taken into account, although it is very small.

[26] The resulting concentrations for CO_2 and CH_4, and the O_3 burden, are shown in Figure 5 for the example of NO_x emissions from the four continental regions. When normalized to a 1 Tg pulse increase in NO_x, the perturbation causes a 1 year increase in ozone and a decrease in methane, which decays away. The increased ozone damage causes an initial rise in carbon dioxide. This rise recovers more rapidly than for a simple CO_2 pulse because the land becomes a net sink of carbon in subsequent years. Hence, the recovery rate is driven more by the evolution of the land carbon storage in JULES than by the shape of the CO_2 impulse response function used in the analytical climate model.

[27] To convert the concentration changes into radiative forcings, the formulas from the work of *Ramaswamy et al.* [2001] are used for carbon dioxide and methane, using baseline concentrations of 380 ppm, 1760 ppb, and 314 ppb for CO_2, CH_4, and N_2O, respectively. The radiative forcing from ozone is estimated from the tropospheric burden using the scaling for the STOCHEM_HadGEM1 model calculated by *Gauss et al.* [2006] of 0.32 W m^{-2} for a 10.9 Dobson unit (DU) change in burden. This is a simplistic assumption because different emission perturbations are likely to result in different geographical and vertical distributions of the ozone response [e.g., *Shindell et al.*, 2005]. However, the uncertainty in the scaling from different chemistry models [*Gauss et al.*, 2006] is comparable to the variation owing to emission type.

3.4. Temperature Impact

[28] The global surface temperature change is derived by convolving the radiative forcing time profiles from section 3.3 with the temperature impulse response function as described in section 2.3. The resulting temperature changes are shown in Figure 6 for the perturbations summed over all the four continental regions used. Again, the results are scaled by the emission changes to give a temperature change in mK/Tg. For NO_x emissions, the temperature change owing to ozone impacts is noticeably smoothed by the temperature response function. The impact of the methane change is of the opposite sign, and, with no carbon cycle impact (black dashed line), the global averaged response to a 1 Tg NO_x pulse emission would be warming for 5 years followed by a cooling. However, when the carbon cycle impact is included, the change in CO_2 is large enough to compensate for the methane cooling for 40 years (high sensitivity) after the NO_x impulse. The reason that the CO_2

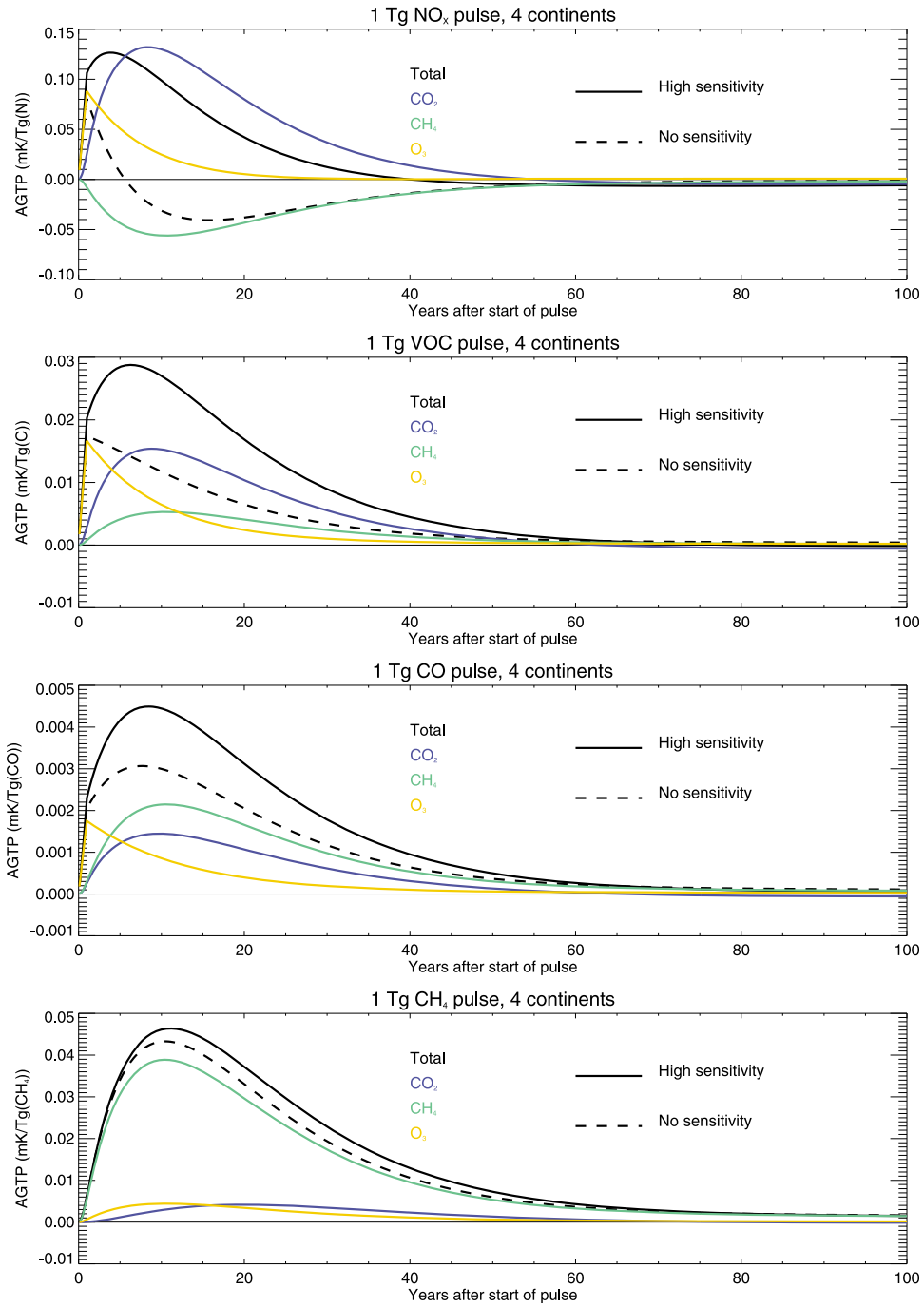

Figure 6. Absolute global temperature potential (mK/Tg) for a 1 year pulse emission of ozone precursors. The normalization is per Tg(N) for NO_x, per Tg(C) for VOCs, per Tg(CO) for CO, and per Tg(CH_4) for CH_4. The solid black line is the sum of all three components (high sensitivity of plants to ozone). The dashed line is the sum of only the ozone and methane components (no sensitivity of plants to ozone).

response does not outlast that of methane is because its response is driven by the adjustment time of the vegetation and soil rather than by the lifetime of CO_2 in the atmosphere. For VOC and CO emission changes, the ozone, methane, and carbon dioxide all act in the same direction (warming for a positive emission change).

[29] To calculate the radiative forcing for the methane experiment, the methane mixing ratio was decreased linearly from 1760 to 1408 ppbv over the first year and then recovered with an e-folding lifetime given by $\tau_0 f$. There is no ozone initial pulse, but the same relationship between methane and ozone was used as before to calculate the long-term ozone response. To normalize the results, we need to calculate an emission reduction equivalent to the 20% mixing ratio change. This equivalent emission works out to be −1020 Tg/yr, which is a factor of 2 larger than the total

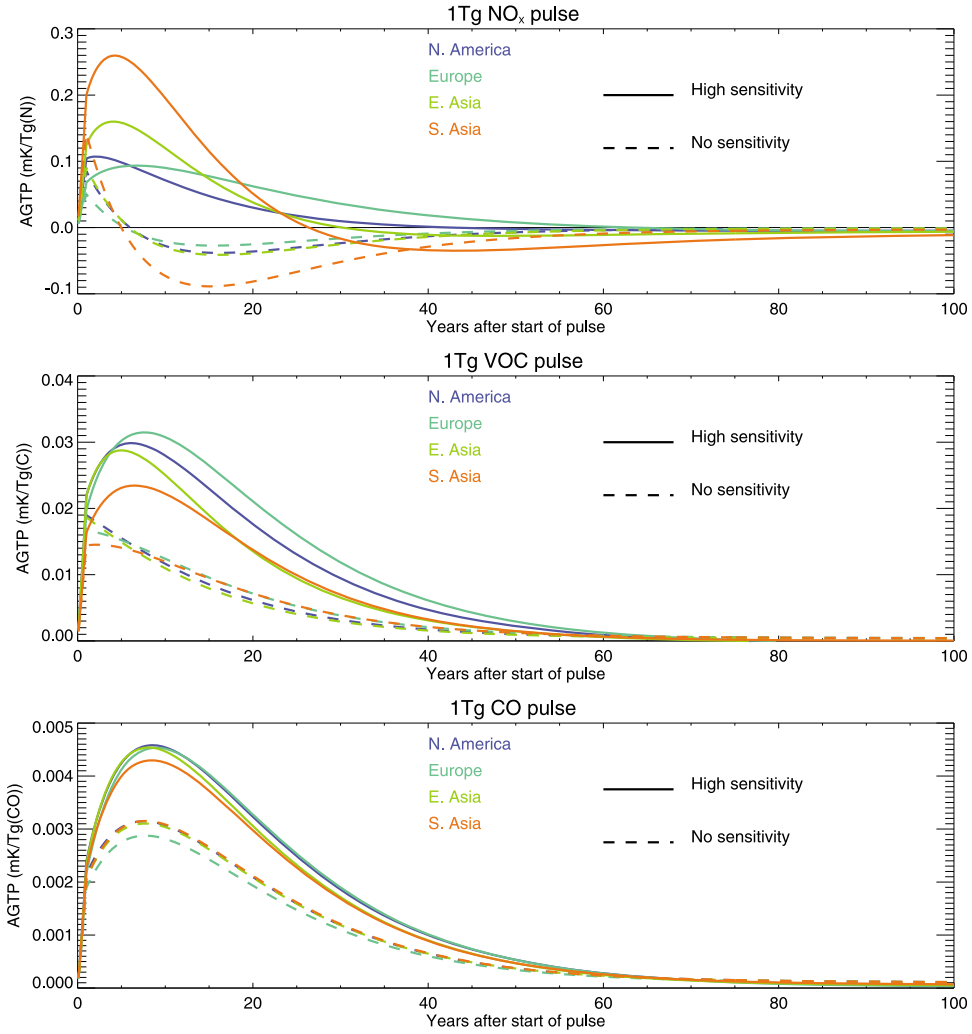

Figure 7. Absolute global temperature potential (AGTP) in mK/Tg for the different emitted species from different regions. The normalization is per Tg(N) for NO_x, per Tg(C) for VOCs, and per Tg (CO) for CO. The solid lines assume a high sensitivity of plants to ozone. The dashed lines assume no sensitivity of plants to ozone.

methane emissions used. This calculation is further justification for using a concentration perturbation rather than emissions for methane. Most of the climate impact comes from the direct effect of the methane itself, with ozone contributing about 10% to the temperature change and the carbon dioxide 10%–20% (high sensitivity) in the central portion of the integration (years 20–70).

[30] It is useful to break down the temperature changes by source region. Figure 7 shows the absolute global temperature potential (AGTP) for 1 Tg emission split by source region and emission species. Solid or dashed lines assume high or no sensitivity, respectively, of the vegetation to CO_2. The sensitivity to location can occur through the efficiency of ozone production, the impact on the methane lifetime, and the proximity of vegetation. This is most obvious for NO_x emissions where initially climate is most sensitive to emissions from South Asia owing to the high ozone production efficiency and proximity to vegetation. However, methane chemistry is most active in the tropics, so ultimately South Asian NO_x has a cooling effect. In the longer term, climate is most sensitive to European NO_x emissions because they have the least impact on the methane lifetime, being farthest away from the tropics. Climate is less sensitive to where VOC and CO emissions are emitted. From Figure 7 (middle) it can be seen for the case of VOC emissions that most of the geographical variation appears in the solid lines, indicating that vegetation damage is causing this variation. This finding is borne out by further analysis.

3.5. Global Temperature Potentials

[31] A useful way to compare the direct and indirect climate contributions is through a normalized metric relating the temperature impacts of an ozone precursor emission to that of CO_2 [*Shine et al.*, 2007]. To do this, we simply divide the temperature response functions in Figure 7 by the equivalent response to a 1 Tg CO_2 pulse emission using the same analytical climate and carbon cycle model as before.

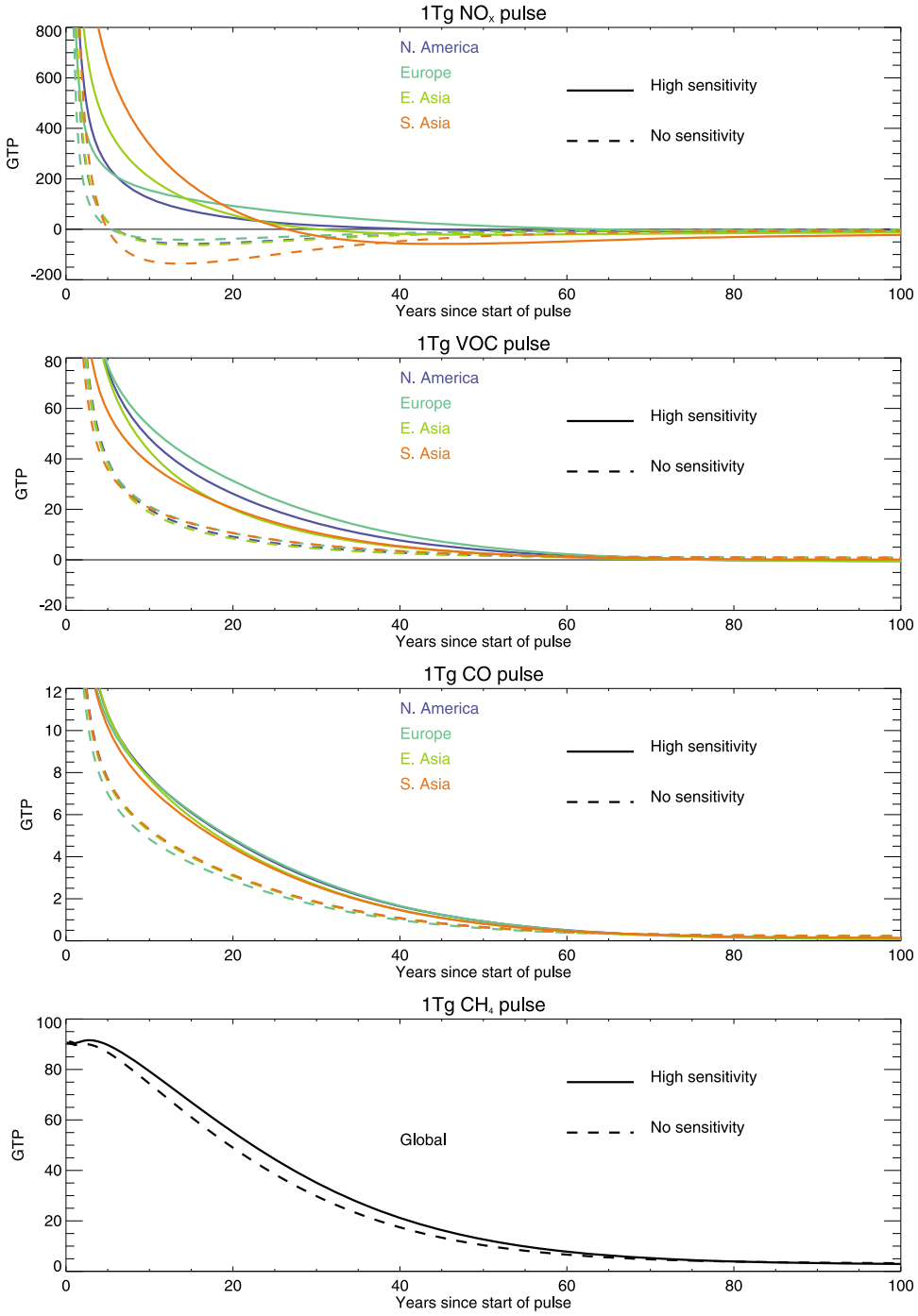

Figure 8. As in Figure 7, but for the GTPs (i.e., normalized by the AGTP for carbon dioxide).

This leads to the GTPs shown in Figure 8 as functions of time since the pulse. Table 3 lists the GTPs at 20 and 50 years; here the values assuming a low sensitivity of plants to ozone are shown as well as for "no" and "high" sensitivity. It is common to quote a GTP_{100} as a comparison with the GWP_{100} commonly used to rank long-lived greenhouse gases; however, for the ozone precursors (other than methane), the GTP_{100} is very small. This reflects the fact that after 100 years any climate signal from the short-lived gases has dissipated. The results from Table 3 are shown graphically in Figure 9. The symbols show the GTPs for the low-sensitivity case, and the whiskers show the range from no sensitivity to high plant O_3 sensitivity.

[32] For NO_x emissions, as we have seen before, there is a large variation in the climate impact of the different source regions. Assuming no sensitivity of plants to ozone, the GTP_{20} values vary from −140 (shipping) to −37 (Europe). Including low or high plant sensitivities changes the signs of

Table 3. GTPs at 20 and 50 Years for Ozone Precursors Emitted in Different Regions[a]

Region	GTP_{20}			GTP_{50}		
	No Sens	Low Sens	High Sens	No Sens	Low Sens	High Sens
N. America NO_x	−53	8	44	−12	−5	−4
Europe NO_x	−37	51	92	−8	5	13
E. Asia NO_x	−57	34	55	−13	−21	−22
S. Asia NO_x	−120	14	75	−27	−43	−57
Four continents NO_x	−56	28	62	−13	−9	−8
Shipping NO_x	−135	−92	−53	−30	−31	−29
N. America VOC	9	20	26	1.8	2.7	3.9
Europe VOC	11	24	31	2.1	3.6	5.0
E. Asia VOC	9	19	20	1.6	1.8	2.5
S. Asia VOC	11	16	20	2.1	2.1	2.5
Four continents VOC	10	20	25	1.9	2.6	3.7
N. America CO	3.1	4.1	4.8	0.6	0.8	0.9
Europe CO	2.8	4.1	4.8	0.6	0.8	0.9
E. Asia CO	3.1	4.1	4.5	0.6	0.7	0.8
S. Asia CO	3.1	3.8	4.4	0.6	0.7	0.8
Four continents CO	3.0	4.0	4.6	0.6	0.7	0.9
Methane	49	52	55	10	11	13

[a]The normalization masses used are (N) for NO_x, (C) for VOCs, (CO) for CO, and (CH_4) for CH_4.

the GTP_{20} values (except for shipping), with values for the continental source regions varying between 46 and 95 for the high-sensitivity case. Shipping, not surprisingly, has the least impact on land carbon, and so the small contribution of the CO_2 changes cannot overcome the large impact on methane from shipping in tropical waters. Even if we assume the highest sensitivity for vegetation, shipping NO_x has a negative GTP after 20 years.

[33] In the high-sensitivity case, the ozone damage increases GTP_{20} by a factor of 2 or more for VOC emissions, by 40%–70% for CO emissions, and by 13% for CH_4 emissions. On the longer timescale, the impact of ozone damage on GTP_{50} is again to increase the values (except for South Asian NO_x), although, for the NO_x emissions, this is only enough to turn the GTP_{50} positive for Europe. Note that the values for VOC emissions are strictly only applicable for the mix of VOC species perturbed here. Results from perturbing any one VOC may give a very different impact [*Collins et al.*, 2002].

[34] For methane, the GTP_{100} values are 3.2, 3.1, and 2.9 for no, low, and high sensitivities. At first sight, this result that damage to vegetation reduces the CO_2 forcing seems counterintuitive. The terrestrial carbon cycle recovers with a roughly 25 year e-folding time. In the absence of other reservoirs, the initial pulse of CO_2 would be taken back up by the vegetation as it recovers, so after 100 years the atmospheric concentration would be almost back to the initial value. However, part of the initial CO_2 pulse is taken up by long-timescale carbon reservoirs (such as the ocean); hence, the drawdown of CO_2 by the recovering vegetation temporarily brings down the atmospheric concentration below its initial value.

[35] For methane, our results with no vegetation sensitivity are similar to, but slightly lower than, those of *Boucher et al.* [2009], who calculated GTPs of 51 and 3.5 for 20 and 100 year time horizons. The Boucher et al. study used a simple scaling of the methane forcing to get the ozone contribution rather than using a chemistry model, as was performed here.

4. Uncertainties

4.1. Neglected Processes

[36] With the model setup we have used, we were able to address many of the indirect climate impacts of ozone precursor emissions through gas-phase photochemistry and ozone damage to vegetation. There are, however, further indirect effects that we have not been able to address. In this section, we use results from the literature to make rough estimates of their contributions to the GTPs in comparison to the results we derived in section 3.5.

4.1.1. Aerosol Interactions

[37] In addition to the impacts on ozone and methane, NO_x emissions can also form ammonium nitrate aerosol. *Bauer et al.* [2007] calculated the climate impact from the direct effect of anthropogenic nitrate aerosol to be 0.06 W m^{-2} from the emission of 29.9 Tg (N) of NO_x. Using this relationship leads to an estimate of a contribution to the GTP_{20} and GTP_{50} of −25 and −4.0, respectively, for the four-continent case. The aerosol-cloud indirect effects add to this contribution.

[38] *Shindell et al.* [2009] found that the sulfur cycle in their model is very sensitive to the OH levels in the atmosphere. In our Met Office HadGEM2 aerosol scheme, the impact of oxidant increases on the sulfate forcing was found to be small [*Rae et al.*, 2007]. A subsequent sensitivity analysis showed that changes in sulfate aerosol (direct effect only) contribute on the order of −3 to the GTP_{20} for NO_x and +2 to the GTP_{20} for methane.

4.1.2. Further Carbon Cycle Processes

[39] Although NO_x emissions damage vegetation through production of ozone, the extra reactive nitrogen deposited can fertilize plant growth and so may to some extent compensate for the ozone damage. As a crude estimate of the magnitude of the impact, we take the numbers from *Hungate et al.* [2009], leading to an uptake of 0.01 Pg(C)/Tg(N). This is approximately 10% of the change in uptake due to the ozone damage, so we can scale the GTPs calculated previously. This gives nitrogen deposition contributions to the "four-continents" NO_x GTP_{20} of around −10. However, this may be considered an upper estimate because the effect of nitrogen fertilization on net carbon balance of terrestrial ecosystems is highly uncertain, and there is some field evidence to suggest a stimulation of both plant and microbial activity under elevated nitrogen conditions [*Neff et al.*, 2002; *Mack et al.*, 2004]; therefore, increases in vegetation carbon may be offset by reductions in soil carbon.

[40] *Mercado et al.* [2009] found an additional climate cooling impact of aerosols through increasing the diffuse fraction of sunlight reaching vegetation. Huntingford et al. [*Huntingford et al.*, 2010] extended this work by calculating a change in land carbon of 0.3 Gt(C) for a 1 W m^{-2} aerosol forcing. Applying this scaling to the nitrate aerosol generated by the four-continent NO_x emissions described earlier in this section would lead to an impact on the GTP_{20} for NO_x of less than 1.

4.1.3. Other Processes

[41] Increased stratospheric water vapor from the oxidation of methane leads to a radiative forcing of approximately

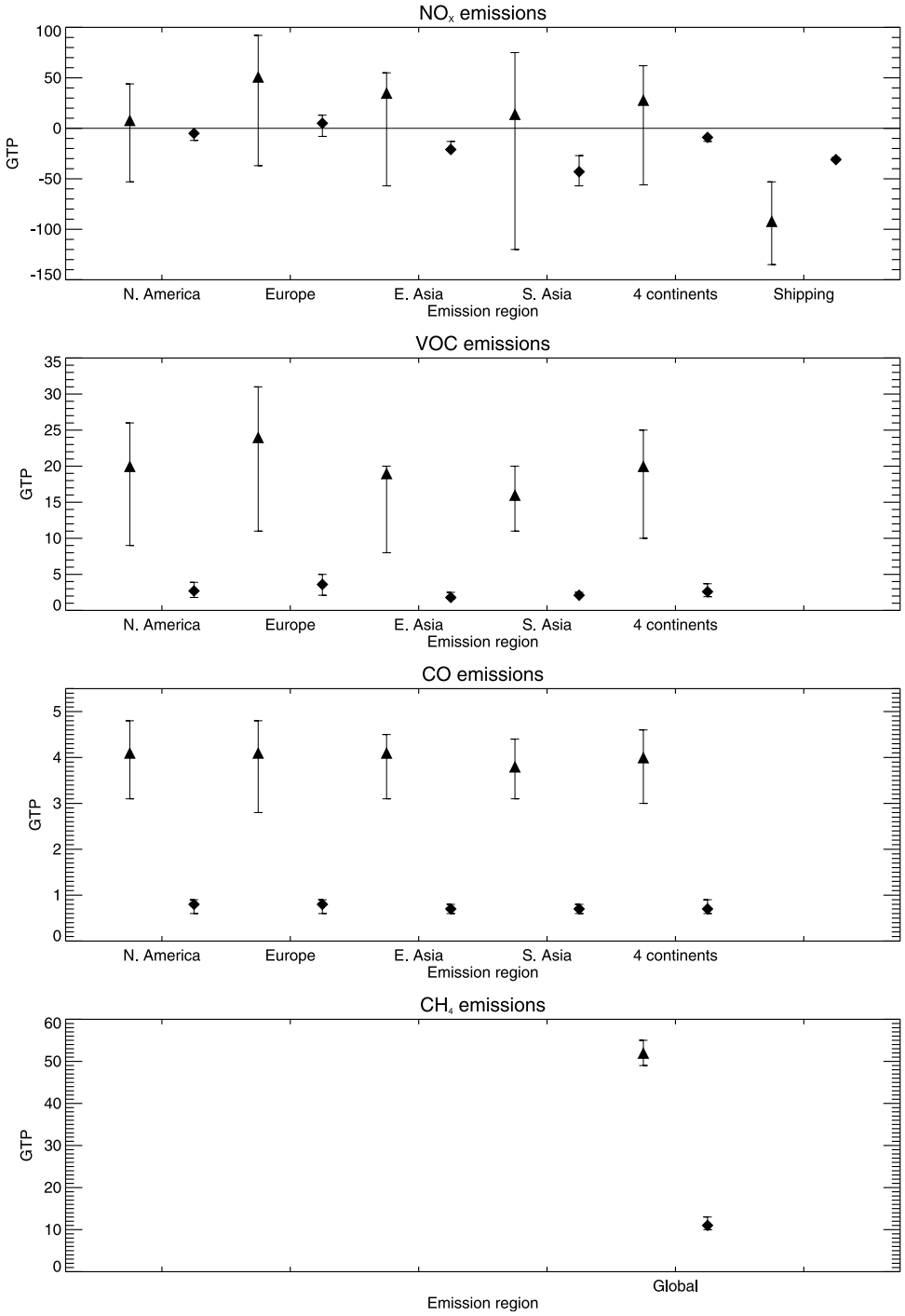

Figure 9. GTPs at 20 years (triangles) and 50 years (diamonds) for ozone precursors from different regions. The central symbol shows the value for low sensitivity to ozone; the whiskers span the range from no sensitivity (bottom) to high sensitivity (top). Note that for the GTP_{50} values for East Asian and South Asian NO_x the ozone damage has a cooling effect, so these two bars should be read as no sensitivity at the top to high sensitivity at the bottom.

15% of the direct methane effect [*Forster et al.*, 2007]. Applying this factor to our results gives an increment to the methane GTPs of 6.1 and 1.3 for 20 and 50 year time horizons, respectively. Because the other ozone precursors also affect methane and hence stratospheric water vapor, we calculated the stratospheric water impacts in the "four-continent" case. The increments are NO_x $\Delta GTP_{20} = -10$, $\Delta GTP_{50} = -3$; VOC $\Delta GTP_{20} = 1$, $\Delta GTP_{50} = 0.2$; CO $\Delta GTP_{20} = 0.4$, and $\Delta GTP_{50} < 0.1$.

[42] *Boucher et al.* [2009] calculated a contribution to the methane GTP from chemical CO_2 production of 1.0–1.9 and 1.4–2.8 for 20 and 100 year time horizons, respectively.

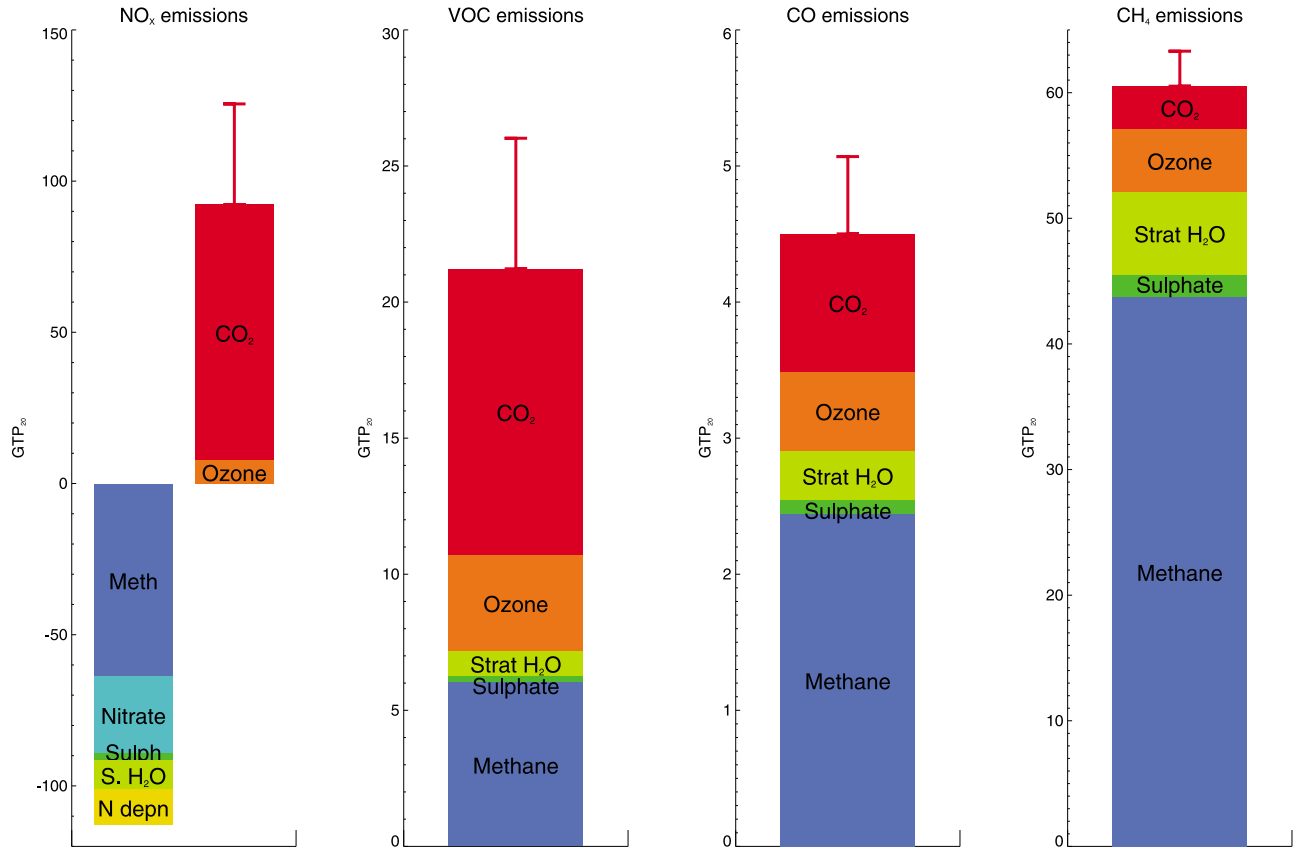

Figure 10. Components contributing to the GTP_{20} values for emissions from the four continental regions: methane, nitrate aerosols, sulfate aerosols, stratospheric water vapor, nitrogen fertilization of vegetation, ozone, and carbon dioxide from reduced vegetation uptake. The whisker on top of the CO_2 bar illustrates the range between the low- and high- sensitivity assumptions. Aerosol indirect effects are not accounted for.

Using the CO_2 production efficiencies from STOCHEM gives increments to the CO and VOC GTPs of 1.1 in both cases and for all time horizons.

4.2. Model Uncertainties

[43] *Fiore et al.* [2009] compared the sensitivities of a range of models to 20% emission perturbations. Differences between models were attributed both to the differences in the model performance and to differences in the absolute emission perturbations applied. They typically found one-standard-deviation uncertainties of 30% in the surface ozone response over the source regions. Variations between the models in the changes to the methane lifetime were of the order of 30%–40%, except for the methane experiment itself, in which the standard deviation in the change in lifetime was 10%.

[44] The uncertainties in the responses of vegetation to ozone are large. Most flux-response assessments that have been made (such as those used in the paper by *Sitch et al.* [2007]) are for crops or for a small number of temperate and boreal tree species. In this study (as in that by Sitch et al.), we used two parameterizations of ozone damage, which we labeled "low" and "high" sensitivities. For broad-leaved trees, these correspond approximately to oak and beech/birch. There are certainly many tree species whose responses could lie outside the range given by those selected by Sitch et al.; hence, the range given in Figure 9 does not give the full picture for the uncertainty. Until more flux-based assessments of the responses to ozone of many more tree species (especially from the tropics) are made, it will be difficult to give a better estimate of the uncertainty.

[45] As discussed in section 3.3, a single number (29 mW m^{-2} DU^{-1}) was used to calculate the radiative forcing from ozone. To gauge roughly the uncertainties associated with this, we took as an example the radiative forcing efficiencies from the work of *Shindell et al.* [2005] (23 and 43 mW m^{-2} DU^{-1} for NO_x- and non-NO_x-induced ozone). This decreases the GTP_{20} values for NO_x by 2 to 3 and increases the GTP_{20} values for VOCs, CO, and methane by 2, 0.3, and 2, respectively. Relative impacts on the GTP_{50} values are smaller. For NO_x, VOCs, and CO, these variations are much smaller than the vegetation damage impact. For methane, the added uncertainties are about two thirds of the low-sensitivity effect or one third of the high-sensitivity effect.

4.3. Total Climate Impact

[46] Adding in the non–carbon cycle processes listed in section 4.1 to the values from section 3.5, we arrive at a total estimate for four-continent emissions of NO_x of $GTP_{20} = -9$ to +24 and $GTP_{50} = -14$ to −12. For methane, the values are GTP_{20} = 61 to 63 and GTP_{50} = 13 to 14, and for CO they are GTP_{20} = 4.5 to 5.1 and GTP_{50} = 0.7 to 0.8. The ranges

are from low to high sensitivity. Although suggesting a possible warming effect, NO_x results bracket zero for the GTP_{20} and are negative for the GTP_{50}. The nitrogen fertilization impact is very uncertain. We suggest that an upper bound to its cooling contribution to the NO_x GTP_{20} might be of the order of −10. The components contributing to the GTP_{20} values are illustrated in Figure 10.

5. Conclusions

[47] We found that on a 20 year timescale the impact of ozone damage to vegetation contributes significantly to the climate impact of ozone precursors by reducing the amount of carbon dioxide taken up by the terrestrial biosphere. We use here the change in global surface temperature as one measure of the climate impact. For NO_x and VOC emissions, the impact on the carbon cycle is the dominant contribution to the induced surface temperature change. Even for methane, the perturbation to the carbon cycle adds approximately 10% to the climate impact. For longer timescales (50 years), the contribution from the ozone damage declines because of the recovery of the vegetation. The climate impact depends strongly on the emission region, both because of the variation in photochemistry and because of the variation in the response of the vegetation.

[48] We have chosen to focus on the GTP measure of climate change over the more commonly used GWP. GTP is an endpoint measure rather than an integral over a time period, so the impacts of the short-lived forcing agents do not persist as long as they do for the GWP. Taking into account the additional processes in section 4.1, we conclude that the sign of the climate impact of NO_x emissions from the four continental regions combined is uncertain for at least the first 20 years after emission, because this is the small residual of large opposing terms from the ozone damage, and the methane and aerosol responses. After less than 50 years, the negative terms dominate (principally the decreased methane), leading to an unambiguous cooling of climate, although this cooling is 30%–40% less than when the ozone damage is not included.

[49] **Acknowledgments.** We wish to thank the three reviewers for their helpful comments on this paper. We are very grateful for the help and advice provided by Chris Huntingford on the carbon cycle modeling, and by Drew Shindell on the aerosol effects. W.J.C. and O.B. were supported by the Joint DECC and Defra Integrated Climate Programme, DECC/Defra (GA01101). W.J.C. was also supported by Defra contract AQ0902.

References

ApSimon, H., M. Amann, S. Åström, and T. Oxley (2009), Synergies in addressing air quality and climate change, *Clim. Policy*, *9*, 669–680.

Bauer, S. E., D. Koch, N. Unger, S. M. Metzger, D. T. Shindell, and D. G. Streets (2007), Nitrate aerosols today and in 2030: A global simulation including aerosols and tropospheric ozone, *Atmos. Chem. Phys.*, *7*, 5043–5059.

Boucher, O., and M. S. Reddy (2008), Climate trade-off between black carbon and carbon dioxide emissions, *Energy Policy*, *36*, 193–200.

Boucher, O., P. Friedlingstein, W. J. Collins, and K. P. Shine (2009), Indirect GWP and GTP due to methane oxidation, *Environ. Res. Lett.*, *4*, 044007, doi:10.1088/1748-9326/4/4/044007.

Collins, W. J., R. G. Derwent, C. E. Johnson, and D. S. Stevenson (2002), The oxidation of organic compounds in the troposphere and their global warming potentials, *Clim. Change*, *52*, 453–479.

Collins, W. J., R. G. Derwent, B. Garnier, C. E. Johnson, M G Sanderson, and D. S. Stevenson (2003), The effect of stratosphere-troposphere exchange on the future tropospheric ozone trend, *J. Geophys. Res.*, *108*(D12), 8528, doi:10.1029/2002JD002617.

Collins, W. J., M. G. Sanderson, and C. E. Johnson (2009), Impact of increasing ship emissions on air quality and deposition over Europe by 2030, *Meteorol. Z.*, *18*(1), 25–39, doi:10.1127/0941-2948/2008/0296.

Cox, P. M. (2001), Description of the TRIFFID dynamic global vegetation model, *Tech. Note 24*, Hadley Cent., Met Off., Exeter, U. K.

Dentener, F., et al. (2006), Nitrogen and sulfur deposition on regional and global scales: A multi-model evaluation, *Global Biogeochem. Cycles*, *20*, GB4003, doi:10.1029/2005GB002672.

Essery, R. L. H., M. J. Best, R. A. Betts, P. M. Cox, and C. M. Taylor (2003), Explicit representation of subgrid heterogeneity in a GCM land surface scheme, *J. Hydrometeorol.*, *4*, 530–543.

Eyring, V., et al. (2007), Multi-model simulations of the impact of international shipping on atmospheric chemistry and climate in 2000 and 2030, *Atmos. Chem. Phys.*, *7*, 757–780.

Fiore, A. M., et al. (2009), Multimodel estimates of intercontinental source-receptor relationships for ozone pollution, *J. Geophys. Res.*, *114*, D04301, doi:10.1029/2008JD010816.

Forster, P. M., et al. (2007), Changes in atmospheric constituents and in radiative forcing, in *Climate Change 2007: The Physical Science Basis. Contribution of Working Group I to the Fourth Assessment Report of the Intergovernmental Panel on Climate Change*, pp. 129–234, Cambridge Univ. Press, Cambridge, U. K.

Gauss, M., et al. (2006), Radiative forcing since preindustrial times due to ozone change in the troposphere and the lower stratosphere, *Atmos. Chem. Phys.*, *6*, 575–599.

Gedney, N., P. M. Cox, R. A. Betts, O. Boucher, C. Huntingford, and P. A. Stott (2006), Detection of a direct carbon dioxide effect in continental river runoff records, *Nature*, *439*, 835–838.

Hungate, B. A., J. S. Dukes, M. R. Shaw, Y. Luo, and C. B. Field (2009), Nitrogen and climate change, *Science*, *203*, 1512–1513.

Huntingford, C., P. M. Cox, L. M. Mercado, S. Sitch, N. Bellouin, O. Boucher, and N. Gedney (2010), Highly contrasting effects of different climate forcing agents on ecosystem services, *Philos. Trans. R. Soc. A*, doi:10.1098/rsta.2010.0314, in press.

Jackson, S. C. (2009), Parallel pursuit of near-term and long-term climate mitigation, *Science*, *326*, 526–527.

Johns, T. C., et al. (2006), The new Hadley Centre Climate Model (HadGEM1): Evaluation of coupled simulations, *J. Clim.*, *19*, 1327–1353.

Karlsson, P. E., et al. (2004), New critical levels for ozone effects on young trees based on AOT40 and simulated cumulative leaf uptake of ozone, *Atmos. Environ.*, *38*, 2283–2294.

Keating, T., and A. Zuber (2007), Hemispheric transport of air pollution 2007, *Air Pollut. Stud. Rep. 16*, UN Econ. Comm. for Eur., Geneva, Switzerland.

Mack, M. C., E. A. G. Schuur, M. S. Bret-Harte, G. R. Shaver, and F. S. Chapin III (2004), Ecosystem carbon storage in Arctic tundra reduced by long-term nutrient fertilization, *Nature*, *431*, 440–443.

Mercado, L. M., N. Bellouin, S. Sitch, O. Boucher, C. Huntingford, M. Wild, and P. M. Cox (2009), Impact of changes in diffuse radiation on the global land carbon sink, *Nature*, *458*, 1014–1018.

Neff, J. C., A. R. Townsend, G. Gleixnerk, S. J. Lehman, J. Turnbull, and W. D. Bowman (2002), Variable effects of nitrogen additions on the stability and turnover of soil carbon, *Nature*, *419*, 915–917.

Olivier, J. G. J., and J. J. M. Berdowski (2001), Global emissions sources and sinks, in *The Climate System*, edited by J. J. M. Berdowski, R. Guicherit, and B. J. Heij, A. A. Balkema, Brookfield, Vt.

Pleijel, H., H. Damielsson, K. Ojanper, L. De Temmerman, P. Hogy, M. Badiani, and P. E. Karlsson (2004), Relationships between ozone exposure and yield loss in European wheat and potato—A comparison of concentration- and flux-based exposure indices, *Atmos. Environ.*, *38*, 2259–2269.

Prather, M., D. Ehhalt, R. Derwent, E. Dlugokencky, E. Holland, I. Isaksen, J. Katima, V. Kirchoff, P. Matson, P. Midgely, and M. Wang (2001), Atmospheric chemistry and greenhouse gases, in *Climate Change 2001: The Scientific Basis: Contribution of Working Group I to the Third Assessment Report of the Intergovernmental Panel on Climate Change*, edited by J. T. Houghton et al., chap. 5, pp. 239–287, Cambridge Univ. Press, Cambridge, U. K.

Price, C., and D. Rind (1992), A simple lightning parameterization for calculating global lightning distributions, *J. Geophys. Res.*, *97*(D9), 9919–9933, doi:10.1029/92JD00719.

Rae, J. G. L., C. E. Johnson, N. Bellouin, O. Boucher, J. M. Haywood, and A. Jones (2007), Sensitivity of global sulphate aerosol production to changes in oxidant concentrations and climate, *J. Geophys. Res.*, *112*, D10312, doi:10.1029/2006JD007826.

Raes, F., and J. H. Seinfeld (2009), New directions: Climate change and air pollution: A bumpy road, *Atmos. Environ.*, *43*, 5132–5133.

Ramaswamy, V., O. Boucher, J. Haigh, D. Hauglustaine, J. Haywood, G. Myhre, T. Nakajima, G. Y. Shi, and S. Solomon (2001), Radiative forcing of climate change, in *Climate Change 2001: The Scientific Basis. Contribution of Working Group I to the Third Assessment Report of the Intergovernmental Panel on Climate Change*, chap. 6, pp. 350–416, Cambridge Univ. Press, Cambridge, U. K.

Sanderson, M. G., C. D. Jones, W. J. Collins, C. E. Johnson, and R. G. Derwent (2003), Effect of climate change on isoprene emissions and surface ozone levels, *Geophys. Res. Lett.*, *30*(18), 1936, doi:10.1029/2003GL017642.

Shindell, D. T., G. Faluvegi, N. Bell, and G. A. Schmidt (2005), An emissions-based view of climate forcing by methane and tropospheric ozone, *Geophys. Res. Lett.*, *32*, L04803, doi:10.1029/2004GL021900.

Shindell, D. T., et al. (2006), Multimodel simulations of carbon monoxide: Comparison with observations and projected near-future changes, *J. Geophys. Res.*, *111*, D19306, doi:10.1029/2006JD007100.

Shindell, D. T., G. Faluvegi, D. M. Koch, G. A. Schmidt, N. Unger, and S. E. Bauer (2009), Improved attribution of climate forcing to emissions, *Science*, *326*, 716–718.

Shine, K. P., T. K. Berntsen, J. S. Fuglestvedt, R. B. Skeie, and N. Stuber (2007), Comparing the climate effect of emissions of short and long lived climate agents, *Philos. Trans. R. Soc. A*, *365*, 1903–1914.

Sitch, S., P. M. Cox, W. J. Collins, and C. Huntingford (2007), Indirect radiative forcing of climate change through ozone effects on the land-carbon sink, *Nature*, *448*, 791–794.

Stevenson, D. S., et al. (2006), Multimodel ensemble simulations of present-day and near-future tropospheric ozone, *J. Geophys. Res.*, *111*, D08301, doi:10.1029/2005JD006338.

O. Boucher and W. J. Collins, Met Office Hadley Centre, Exeter EX1 3PB, UK. (bill.collins@metoffice.com)

S. Sitch, School of Geography, University of Leeds, Leeds LS2 9JT, UK.